Journal of Non-Crystalline Solids 535 (2020) 119967

Contents lists available at ScienceDirect

Journal of Non-Crystalline Solids

journal homepage: www.elsevier.com/locate/jnoncrysol

Ultrasonic vibration accelerated aging in La-based bulk metallic glasses

Siyuan Chen[a], Song Li[b,*], Jiang Ma[c], Haibin Yu[d], Huashan Liu[a,*], Hailong Peng[a,*]

[a] School of Materials Science and Engineering, Central South University, Changsha 410083, China
[b] State Key Laboratory for Powder Metallurgy, Central South University, Changsha 410083, China
[c] College of Mechatronic and Control Engineering, Shenzhen University, Shenzhen 518060, China
[d] Wuhan National High Magnetic Field Center, Huazhong University of Science and Technology, Wuhan 430074, China

ARTICLE INFO

Keywords:
Bulk metallic glasses
Ultrasound vibration
Aging
Annealing
Thermodynamics

ABSTRACT

The effect of ultrasonic vibrations on the thermodynamic properties of $La_{68.5}Al_{14}Ni_{16}Co_{1.5}$ bulk metallic glasses is systematically studied at various temperatures. We find a significant enthalpy lowering for the glasses after the ultrasonic treatment, due to the structural relaxation towards lower energetic states, coinciding with the finding that the pretreated samples have a noticeable higher energetic barrier for glass transition. With increasing the ultrasound-treating time, the reduced enthalpy saturates in the long-time regime, which is reachable by the isothermal annealing. Based on these results, we conclude that the ultrasonic vibration has, qualitatively, the same effect as that of the annealing process. This is interpreted by the fact that the ultrasonic perturbation is weak for the technique we utilized, and most of the atoms could linearly respond to it. The ultrasound-accelerated aging has also been shown on the aspect of the hardness that was monotonically enhanced with the treating time.

1. Introduction

Owing to the disordered structure in the atomic level, bulk metallic glasses (BMGs) possess unique chemical and physical properties and attract tremendous interests in the research [1–6]. The out-of-equilibrium nature of amorphous state, on the other hand, enables the systems evolves with time, mostly towards low energy configurations, as seen in the phenomenon of physical aging common to all sorts of glasses [7,8]. For instance, annealing is a conventional way to make materials gradually go down to a more stable and lower energy state [9,10]. A smart choice of the protocol that changes the thermodynamic history of the fabricated samples, can inversely levitate the energy of the samples, e.g., recovery annealing above glass transition temperature and cryogenic thermal cycling [11,12].

Recently, external fields are more and more frequently utilized to tune the energetic state of amorphous solids, tailoring the mechanical properties of BMGs. Among them, a novel method is imposing a cyclic loading either locally with nanoindentation or globally with compression or tension [13–15]. It is revealed that elastic cycling by either method relaxes the sample into more stable states and induces hardening. The elastic strain plays a role when it exceeds a threshold, and the hardening saturates with the increasing of cycling number [13,16]. This can be understood in the view of structural heterogeneity which supposes that BMGs consist of weakly bonded regions and strongly bonded regions [17]. Even in the regime the materials macroscopically exhibiting linear respond to external force, there exits locus, i.e., the weakly bonded regions, plastically deformed. This conjecture has been verified both on computer simulations and experiments [14,18]. Beyond the elastic regime, larger strain amplitude could oppositely rejuvenate metallic glasses [19,20].

Comparing to the oscillatory mechanical fields, ultrasonic actuation can “shake” the atoms microscopically with a much higher frequency and an associated wavelength, agitating soft regions in metallic glasses. Thus, it can be used to detect the internal feature of metallic glasses. The effect of ultrasonic excitation on the mechanical behavior of BMGs, in terms of elastic constants, was firstly studied by electromagnetic acoustic resonance [21]. Later, crystallization of Pd-based BMGs was reported under the glass transition temperature caused by ultrasound, with the crystallization time significantly shortened [22]. Based on the spatially resolved crystalline phase that induced by ultrasonic vibration, a heterogeneous structural model for metallic glasses has been proposed [17].

Shaking effect of ultrasonic vibration provides atoms with an additional driving force to explore more energetic metabasins in the potential energy landscape that the atoms usually cannot achieve under thermal activation in the amorphous state. This enables the application of ultrasound as a wetting mechanism by accelerating the atomic diffusion in the interface in BMGs [23], as well as additive manufacturing

* Corresponding authors.
E-mail addresses: ls2011sl@csu.edu.cn (S. Li), hsliu@csu.edu.cn (H. Liu), hailong.peng@csu.edu.cn (H. Peng).

https://doi.org/10.1016/j.jnoncrysol.2020.119967
Received 18 December 2019; Received in revised form 10 February 2020; Accepted 13 February 2020

methods for bulk metallic glasses [24,25]. Resorting to this technique, properties of BMGs can also be refined. It has been reported that the hardness and elastic modulus can be improved after ultrasonic treatment, as well as that of thermal stability in Zr-based BMGs [26]. With ultrasonic actuation that of stronger effect, the local structure on the surface of metallic glasses can be inversely rejuvenated [27].

Regarding to all these interests for studying the physics and material application with the ultrasound technique in metallic glasses, we focus on the evolution of thermodynamic properties for the samples pretreated by ultrasonic vibration at various temperatures. We choose $La_{68.5}Al_{14}N_{i16}Co_{1.5}$ bulk amorphous alloy as a prototype for BMGs, due to its low glass transition temperature and relative good thermal stability [28]. With this merit, we systematically investigated the temperature range from room temperature to its glass transition point at which the ultrasound was applied on the samples. The resulting thermodynamic properties measured by differential scanning calorimetry and the hardness of the samples at room temperature were studied.

2. Experiments

Metallic alloy with a nominal composition of $La_{68.5}Al_{14}Ni_{16}Co_{1.5}$ (at.%) was prepared by arc-melting high-purity elements (> 99.9 wt.%) in a Ti-gettered Ar atmosphere. The ingot was remelted more than 5 times to ensure uniform chemical composition. Then the melt was sucked into a copper mould to form the as-cast rods with the diameter of 2 mm. Slices with the thickness of about 1 mm were cut down from the rod by a water-cooled low-speed diamond cutter in an ethanol solution, and subsequently used for the ultrasound treatment in a heat bath. H201 methylsilicone fluid was used for the heat transfer and sound-wave conduction in the bath at the temperature range from 30 ℃ to 150 ℃. The metallic slices were placed about 0.5 cm down to the ultrasonic sonotrode that emits an acoustic wave with the frequency of 28 kHz at the power of 300 W, at a set of target temperatures. Illustration of how the sample is treated by the ultrasound is shown in Fig. 1. For each selected temperature, we conducted ultrasound treatment for two-time intervals, i.e., 30 mins and 60 mins. Afterwards, the samples were cooled down to the room temperature for further measurements.

The structure of samples were examined by X-ray diffraction (XRD, Rigaku D max 2500 VB with Cu-Kα radiation), and transmission electron microscopy (TEM, JEM-2100F, 200 kV). After the ultrasonic treatment, bulk samples were mechanically ground into thin slices with the thickness about 1∼5 micrometers. Then, the thin slices were used to prepare the specimens for TEM measurement via ion milling (Gatan 691) under liquid nitrogen cooling. Thermal properties were measured by differential scanning calorimeter (DSC, Perkin Elmer 8000) at a heating rate of 20 K/min. The hardness test was carried out by a diamond Berkovich indenter at a maximum load of 30 mN and a loading rate of 1 mN/s. At least 5 times tests were conducted for each measured condition to get the final average values of the hardness.

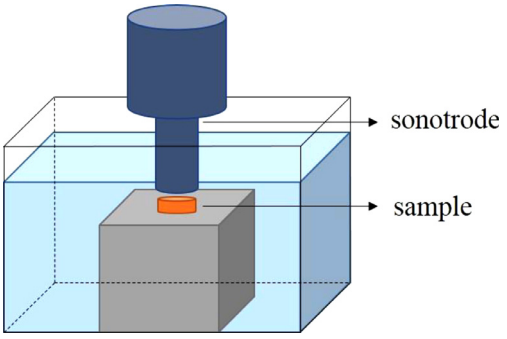

Fig. 1. Illustration of how the sample treated by the ultrasound. Terminal of the ultrasonic sonotrode and the sample are immersed in the liquid, which is used for thermal bath and conducting vibrational waves.

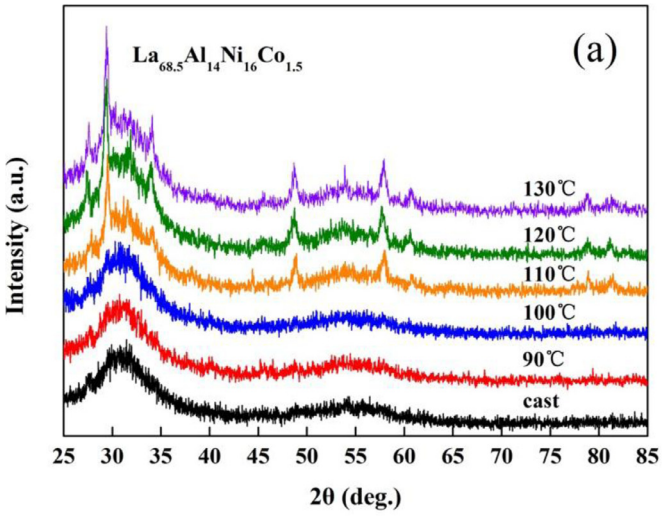

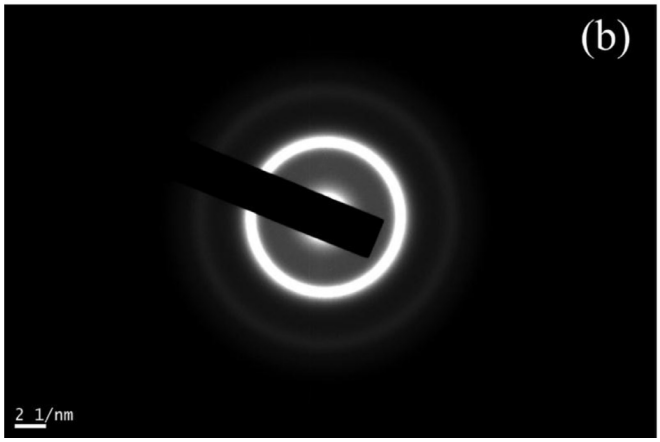

Fig. 2. (a) XRD patterns for the as-cast and the ultrasound-treated $La_{68.5}Al_{14}Ni_{16}Co_{1.5}$ metallic glasses at different temperatures. (b) TEM diffraction pattern for the alloys ultrasound-treated at 100 ℃.

3. Results and discussion

As both isothermal annealing and ultrasound treatment at temperatures below the glass transition point could cause crystallization [17,22,29], it is necessary to examine phase stability of the samples after ultrasonic treatment at various temperatures. Sharp diffraction peaks can be found on the samples with the treatment at 110℃ and above, indicating crystallization happens inside (Fig. 2(a)). In the temperature below, no clear clue is shown for the crystalline phase. There is a broad peak for the scattering angle, 2θ, between 25° and 35°, corresponding to the structure of the first neighbor shell, or the atomic interaction distance in amorphous state. A large value shift of 2θ has been found in the isothermal annealing case with the temperature, indicating the structural densification in Ti-based metallic glasses [29]. But we do not find any significance for similar shift in the La-based metallic glasses. It is possible that there could be some nanocrystalline phase in the amorphous matrix that is difficult for X-ray diffraction to detect [30]. For this sake, we use the TEM as a supplementary method to verify the disordered structure of the samples. As shown in Fig. 2(b), there is no observable light spots in the diffraction pattern, confirming the amorphous state. The isothermal annealing has the probability to induce nanometric sized crystalline grains, then a long-range ordered structure emerges [31]. This structural change is both temperature and composition dependent. Up to 100℃, we do not find any significant

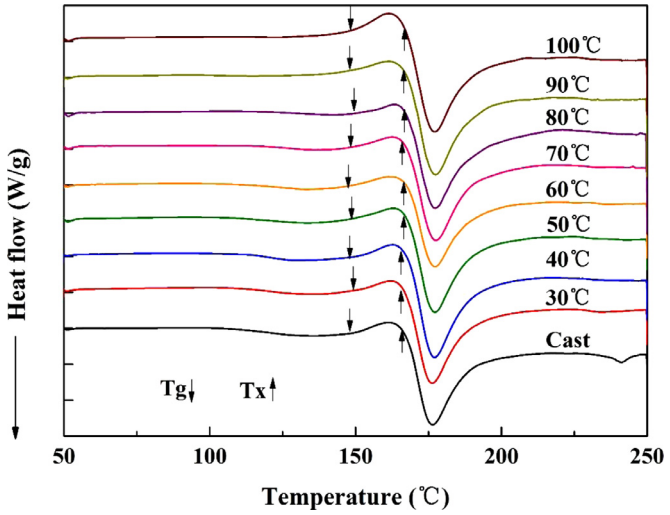

Fig. 3. DSC curves for the as-cast and the ultrasound-treated alloys at a variety of temperatures at a heating rate of 20 K/min.

structural change after the ultrasonic treatment in this metallic glass.

As the amorphous state can only be sustained up to 100℃ from the XRD tests, we measured the thermodynamic properties of the samples pretreated by ultrasound at this point down to room temperature. The DSC curves in Fig. 3 show the heat flow at a heating rate of 20 K/min for the treating time of 30 mins. Isothermal annealing could shift the glass transition temperature, T_g, and crystallization onset temperature, T_x, and then change the thermal stability evaluated as the supercooled liquid region, T_x - T_g, as reported in Zr-based and Ti-based BMGs [29,32,33]. For this alloy, T_x and T_g are found to be around 147℃ and 166℃ from the as-cast curve. They do not exhibit any perceptible changes after pretreatment even at temperature as high as 100℃ (see arrows in Fig. 3). This observation indicates that the macroscopic characteristics of this BMG was not changed under ultrasound pretreatment, consistent with the case of isothermal annealing in La-based metallic glasses [34]. On the as-cast curve, a distinguishable valley emerges at the temperature before T_g, i.e., an exothermic process just before glass transition, which has been well-known to be the annihilation of free volume that frozen in the alloy [35,36]. The annealing process can induce the diminution of defects in the amorphous structure those in the form of pseudo-location dipoles and free volumes as that reported in Fe-based metallic glasses with vibration magnetometer method [36,37]. With the pretreatment temperature going up, this exothermic effect becomes more and more weak and eventually disappears at about 90 ℃.

To illustrate how this exothermic effect canbe affected by the ultrasonic treatment, we select three temperatures for the comparison of DSC curves between the case of ultrasound treatment and isothermal annealing in Fig. 4. At low temperatures ($\leq$ 80 ℃), the thermal flow is mainly influenced in the exothermic regime: curves for both cases show the process of free volume annihilation with the ultrasonic treatment of stronger effect. While for endothermal peaks between T_g and T_x, they almost keep the same shape as that of the as-cast one, indicating the relaxation process happened in the alloy is the reduction of the frozen free volume in the view of free volume theory [34]. At 100 ℃, the exothermal effect disappears, and the endothermal peaks are significantly enhanced comparing to the as-cast curve in both situations. The ultrasonic treatment, again, is of stronger effect. This can be interpreted as the metallic glasses relaxed into configurations that of lower energy than the state the normal thermal history can drive the system into, then more free volumes need to be created during the glass transition, displaying a higher overshoot in DSC curves. The overshoot phenomenon has been commonly observed in the annealing process of BMGs [38,39].

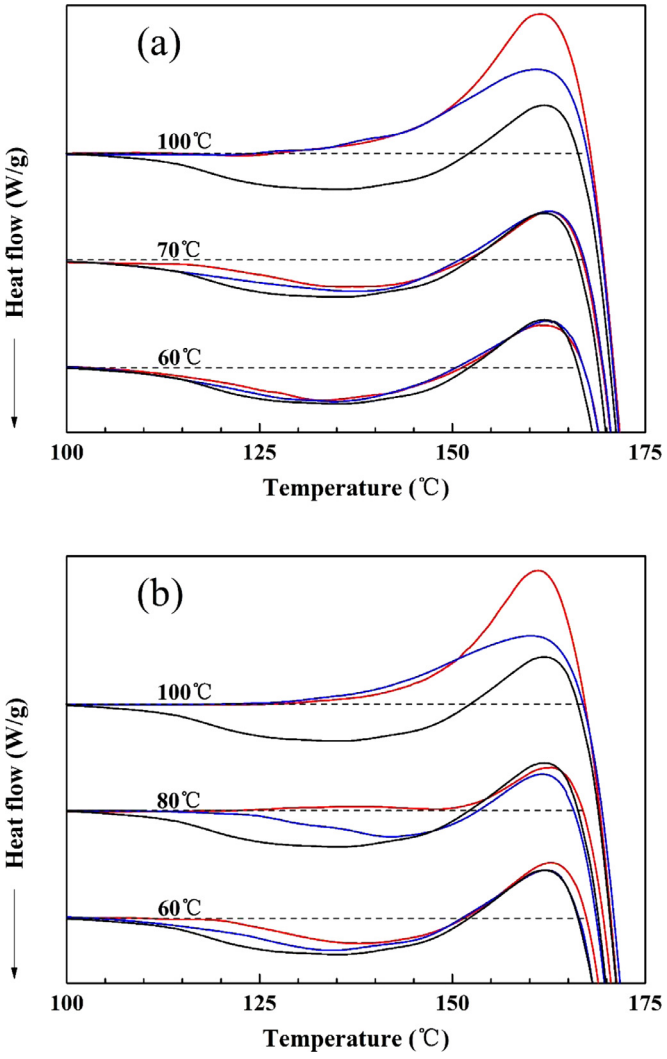

Fig. 4. DSC curves for the annealed and the ultrasound-treated alloys at different temperatures for the treating time of 30 mins at (a), and 60 mins at (b). The black lines are the as-cast curves, the blue lines are the annealing curves, and the red lines are the ultrasound-treated. For clarity, curves at different temperatures are shifted along *y*-axis.

Heat released for BMGs from glass state to supercooled liquid can be calculated from the DSC curve by: $H = \int_{T_0}^{T_e} qdT$, where T_0 (=100 ℃) is the start temperature that the free volume annihilation begins and T_e is the end temperature of glass transition. To evaluate how deep the energetic state the alloys can relax into, we calculate the enthalpy difference: $\Delta H = H - H_0$, with H_0 the as-cast enthalpy. The enthalpy difference for the annealing and the ultrasonic treatment is shown in Fig. 5. Upon the annealing or the ultrasonic treatment, the enthalpy difference is positive, indicating more heat absorption needed for the transition to supercooled state, or to say, a lower enthalpy state of the pretreated glasses. At temperatures up to 80 ℃, the enthalpy difference moderately increases with the temperature, due to the free volume annihilation in the exothermal effect as shown in Fig. 4. At this temperature above, a drastic increment is observed, ascribing to the enhanced endothermal effect around the glass transition temperature. It is plausible that the sharp increase around 80℃ is related to the relaxation transition from the low-temperature beta to the high-temperature alpha relaxation mode as that has been reported in the isothermal annealing process measured by flash DSC [40]. We find both the annealing and the ultrasonic treatment consistently show the same sharp increment at 80℃, with the latter of stronger effect. Thus, in the temperature range

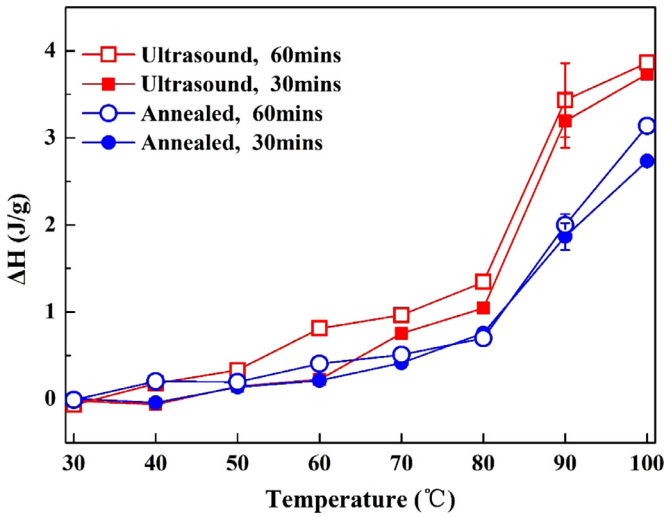

Fig. 5. Enthalpy difference for the annealing case and the ultrasound-treated case at different temperatures.

investigated, the underlying relaxation processes activated by the ultrasonic treatment are the same as those by the isothermal annealing, only with quantitively difference. We verified this observation by a pretreatment duration of 60 mins that shows a coinciding result as that of 30 mins.

To further study the relaxation kinetics, we studied the heating-rate dependent behaviour of the thermal temperatures, T_g and T_x, those responsible for the activation processes of glass transition and crystallization. A common approach to estimate the activation energy of any physical process, for the example of the glass transition, is Moynihan method [41,42]:

$$\frac{d\ln\phi}{d(1/T_g)} = -\frac{E_g}{R}$$

where ϕ is the heating rate, E_g is the activation energy for the glass transition, and R is the gas constant. For the purpose of validation, we also utilized the Kissinger equation to describe the heating-rate dependent glass transition temperature [43]:

$$\frac{d\ln(\phi/T^2)}{d(1/T_g)} = -\frac{E_g'}{R}$$

where E_g' is the activation energy from this method. Illustrations for the fitting of the heating-rate dependent T_g and T_x at 90 °Careshown in Fig. 6(a) and (b) via Moynihan and Kissinger method respectively. The experimental results show nice correspondence for both fittings. These two methods give almost the same values for the fitting parameters, i.e., the activation energies, for all the cases fitted. For briefness, we only show one of the fitting results in Fig. 6(c). For the process of the crystallization, the activation energy almost keeps constant with the pretreatment temperature, indicating the annealing or the ultrasonic vibration cannot affect the crystallization behaviour of the BMGs. For the glass transition process, the activation energy barrier is enhanced by the annealing and the ultrasound, with the effect becoming more and more evident with the temperature. The ultrasonic treatment systematically shows a higher energy barrier than that of the annealing. Thus, the ultrasound vibration can accelerate the structural relaxation and make the system jump into a deeper energy minimum, consistent with the enthalpy state of the samples (see Fig. 5).

Having elucidated the temperature dependence, we turn to the study of the time effect. We conducted the ultrasonic vibration on the alloys at 90 ℃ with various treating times. The enthalpy difference relative to the as-cast one measured by DSC is shown in Fig. 7. It monotonically increases with the treating time, showing a tendency of

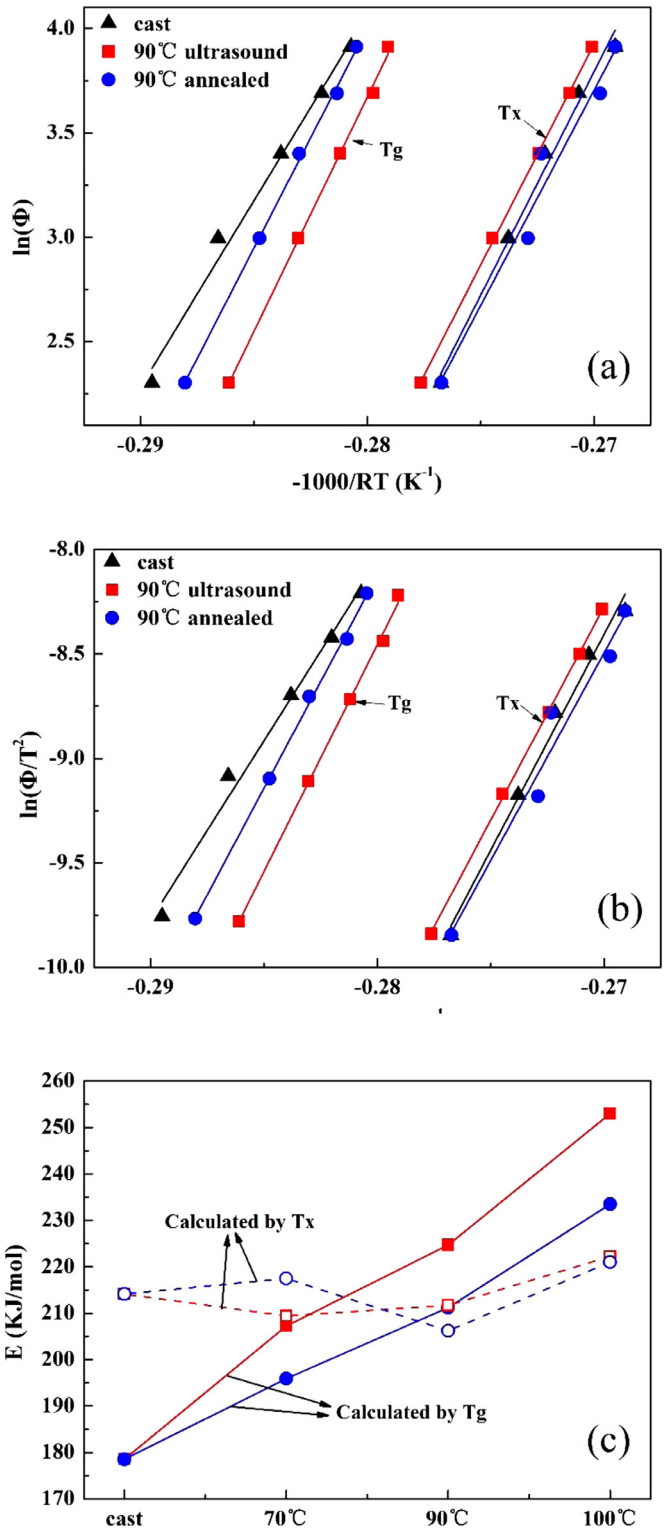

Fig. 6. The heating-rate dependent glass transition and crystallization temperatures, with the Moynihan and the Kissinger fitting in (a) and (b) respectively. (c) is the fitting result for the activation energy in the case of Moynihan method. The solid lines with filled symbols are the activation energy for the glass transition, while the blue lines with hollowed symbols are the ones for the crystallization. Circles are for the treating time of 30 mins, with squares for 60 mins.

saturation at the long-time regime, i.e., longer than 60 mins. The saturation phenomenon can be interpreted as the ultrasound can only shake the atoms in the local energy basin at a small vibrational

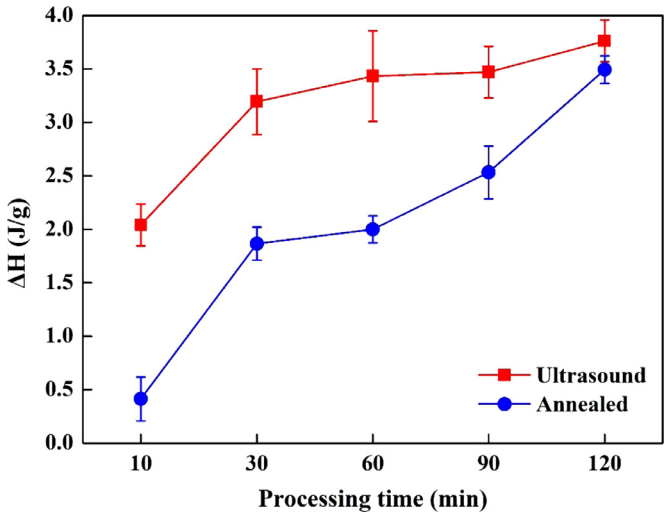

Fig. 7. Change of enthalpy difference for the annealed and the ultrasound-treated alloys pretreated at 90 ℃ with the treating duration.

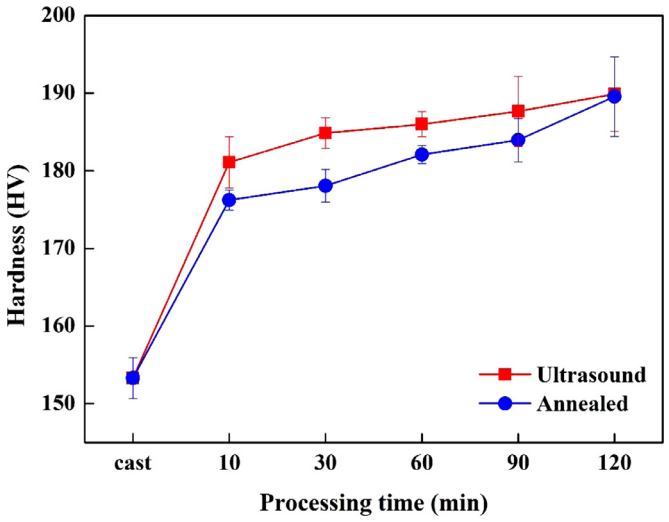

Fig. 8. Change of hardness with the treating time at 90 ℃.

amplitude, which limits the range of the minimum energetic states that the system can explore. The amazing thing is that the annealing seems to approach the ultrasonic state when the annealing time is long enough. This, again, indicates the fact that the ultrasound vibration only quantitively differs from the annealing effect in this study. It is due to the small power of the ultrasound technique utilized here, where most of the atoms still linearly responds to the external field. Works of experiments and computer simulations with the strains exceeding the yield point, have already shown that an oscillatory strain can rejuvenate the system, an effect different from the annealing but not observed here [20,44,45].

The hardness of the pretreated alloys with the treating time is shown in Fig. 8. The micro-hardness exhibits a quick increase with the treating time both by the annealing and the ultrasonic treatment, with a bigger enhancement for the latter at all the points except for the treating time of 120 mins. There is a jump at the time of 10 mins, indicating both the annealing and the ultrasound can significantly enhance the hardness in short time, but much weaker effect in longer time. Nevertheless, the enhancement of the hardness indicates the pretreated alloys are in a relaxed structure of low potential energy, coinciding with the results of thermodynamic measurements.

4. Conclusions

In this paper, the evolution of the enthalpy, the activation energy and the hardness of the La-based bulk metallic glasses before and after the ultrasound treatment at various temperatures and treating times have been investigated. It is found that the ultrasound can accelerate the structural relaxation process of these metallic glasses at the temperatures below 100 ℃, above which the crystallization happens. The enthalpy exhibits a sharp change at around 80 ℃, ascribed to the accelerated relaxation to the energetic state lower than the one the normal thermal procedure can arrive at. The measured activation energy of the glass transition shows an increasing tendency with the pretreating temperature, consistent with the lower enthalpy found. All these ultrasonic effects we found, however, only quantitatively differs from the isothermal annealing effect, without any qualitative difference. We ascribe it to the linear respond of the atoms under the ultrasound treatment by the technique we utilized.

Credit author statement

Siyuan Chen: Performing experimental measurement, data analysis.
Song Li: Supervising DSC measurement, writing.
Jiang Ma: Providing bulk metallic glass samples.
Haibin Yu: Help on sample fabrication.
Huashan Liu: Supervising mechanical property measurement, writing.
Hailong Peng : Project design and management, writing.

Declaration of Competing Interest

None.

Acknowledgments

This work was financially supported by the National Natural Science Foundation of China (under Grant No. 11804394 and Grant No. 51871245).

Supplementary materials

Supplementary material associated with this article can be found, in the online version, at doi:10.1016/j.jnoncrysol.2020.119967.

References

[1] C.A. Schuh, T.C. Hufnagel, U. Ramamurty, Acta Mater. 55 (2007) 4067–4109.
[2] M.D. Demetriou, M.E. Launey, G. Garrett, J.P. Schramm, D.C. Hofmann, W.L. Johnson, R.O. Ritchie, Nature Mater. 10 (2011) 123–128.
[3] W.L. Johnson, G. Kaltenboeck, M.D. Demetriou, J.P. Schramm, X. Liu, K. Samwer, C.P. Kim, D.C. Hofmann, Science 332 (2011) 828–833.
[4] W.H. Wang, C. Dong, C.H. Shek, Mater. Sci. Eng. R 44 (2004) 45–89.
[5] R.V. Belosludov, A.I. Oreshkin, S.I. Oreshkin, D.A. Muzychenko, H. Kato, D.V. Louzguine-Luzgin, J. Alloy. Comp. 816 (2020) 152680.
[6] J.J. Kruzic, Adv. Eng. Mater 18 (2016) 1308–1331.
[7] I.M. Hodge, Science 267 (1995) 1945–1947.
[8] W.H. Wang, Prog. Mater. Sci. 106 (2019) 100561.
[9] L. Hu, C. Zhou, C. Zhang, Y. Yue, J. Chem. Phys 138 (2013) 174508.
[10] W. Dmowski, C. Fan, M.L. Morrison, P.K. Liaw, T. Egami, Mater. Sci. Eng. A 471 (2007) 125–129.
[11] J. Saida, R. Yamada, M. Wakeda, Appl. Phys. Lett 103 (2013) 221910.
[12] S.V. Ketov, Y.H. Sun, S. Nachum, Z. Lu, A. Checchi, A.R. Beraldin, H.Y. Bai, W.H. Wang, D.V. Louzguine-Luzgin, M.A. Carpenter, A.L. Greer, Nature 524 (2015) 200–203.
[13] C.E. Packard, L.M. Witmer, C.A. Schuh, Appl. Phys. Lett 92 (2008) 171911.
[14] C. Deng, C.A. Schuh, Appl. Phys. Lett 100 (2012) 251909.
[15] N. Al-Aqeeli, J. Alloys Comp. 509 (2011) 7216–7220.
[16] D.V. Louzguine-Luzgin, V.Yu. Zadorozhnyy, S.V. Ketov, Z. Wang, A.A. Tsarkov, A.L. Greer, Acta Mater. 129 (2017) 343–351.
[17] T. Ichitsubo, E. Matsubara, T. Yamamoto, H.S. Chen, N. Nishiyama, J. Saida, K. Anazawa, Phys. Rev. Lett. 95 (2005) 245501.
[18] W. Dmowski, T. Iwashita, C.-.P. Chuang, J. Almer, T. Egami, Phys. Rev. Lett. 105 (2010) 205502.

[19] F.O. Méar, B. Lenk, Y. Zhang, A.L. Greer, Scr. Mater. 59 (2008) 1243 – 1246.
[20] K.M. Flores, E. Sherer, A. Bharathula, H. Chen, Y.C. Jean, Acta Mater. 55 (2007) 3403 – 3411.
[21] T. Ichitsubo, S. Kai, H. Ogi, M. Hirao, K. Tanaka, Scr. Mater. 49 (2003) 267 – 271.
[22] T. Ichitsubo, E. Matsubara, K. Anazawa, N. Nishiyama, M. Naito, Y. Hirotsu, Mater. Sci. Eng. A 442 (2006) 273 – 277.
[23] Z. Xu, Z. Li, S. Zhong, Z. Ma, J. Yan, Ultrason. Sonochem. 48 (2018) 207 – 217.
[24] J. Ma, C. Yang, X. Liu, B. Shang, Q. He, F. Li, T. Wang, D. Wei, X. Liang, X. Wu, Y. Wang, F. Gong, P. Guan, W. Wang, Y. Yang, Sci. Adv. 5 (2019) EAAX7256.
[25] W. Wu, J. Jiang, G. Li, J.Y.H. Fuh, H. Jiang, P. Gou, L. Zhang, W. Liu, J. Zhao, J. Non-Cryst, Solids 506 (2019) 1 – 5.
[26] Y. Wang, W. Zhao, G. Li, R. Liu, J. Alloys Comp 544 (2012) 46 – 49.
[27] D.P. Wang, Y. Yang, X.R. Niu, J. Lu, G.N. Yang, W.H. Wang, C.T. Liu, Phys. Rev. B 95 (2017) 235407.
[28] H.B. Yu, X. Shen, Z. Wang, L. Gu, W.H. Wang, H.Y. Bai, Phys. Rev. Lett. 108 (2012) 015504.
[29] X. Wang, P. Gong, L. Deng, J. Jin, S. Wang, F. Li, J. Non-Cryst, Solids 473 (2017) 132 – 140.
[30] M.M.J. Treacy, K.B. Borisenko, Science 335 (2012) 950 – 953.
[31] M. Nabialek, J. Aolly. Comp 642 (2015) 98 – 103.
[32] W.H. Wang, R.J. Wang, W.T. Yang, B.C. Wei, P. Wen, D.Q. Zhao, M.X. Pan, J. Mater. Res. 17 (2002) 1385 – 1389.
[33] J. Gu, M. Song, S. Ni, S. Guo, Y. He, Mater. Des. 47 (2013) 706 – 710.
[34] U. Ramamurty, M.L. Lee, J. Basu, Y. Li, Scr. Mater. 47 (2002) 107 – 111.
[35] A. Slipenyuk, J. Eckert, Scr. Mater. 50 (2004) 39 – 44.
[36] K. Bloch, M. Nabialek, J. Gondro, Physica B 512 (2017) 81 – 84.
[37] M. Nabialek, B. Jez, K. Jez, Rev. Chim. 69 (2018) 2546.
[38] H.J. Jin, J. Wen, K. Lu, Acta Mater. 53 (2005) 3013–3020.
[39] J.C. Qiao, J.M. Pelletier, Intermetallics 19 (2011) 9 – 18.
[40] L. Song, W. Xu, J. Huo, J.-.Q. Wang, X. Wang, R. Li, Intermetallics 93 (2018) 101 – 105.
[41] C.T. Moynihan, J. Am. Ceram, Soc. 76 (1993) 1081 – 1087.
[42] C.T. Moynihan, P.K. Gupta, J. Non-Cryst, Solids 29 (1978) 143 – 158.
[43] H.E. Kissinger, J. Res, Natl. Bur. Stand 57 (1956) 217 – 221.
[44] R. Bhowmich, R. Raghavan, K. Chattopadhyay, U. Ramamurty, Acta Mater. 54 (2006) 4221 – 4228.
[45] Z.-.Y. Zhou, H.-.L. Peng, H.-.B. Yu, J. Chem. Phys. 150 (2019) 204507.